Exploring the Oxygen Evolution Electrocatalysis of an Amine-Based Cobalt Metal-Organic Framework

Jade Nadine S. Ang, Manjunath Chatti, Khang N. Dinh, Stuart R. Batten,* Alexandr N. Simonov* and David R. Turner*

Supporting Information

Contents

1. Analytical Data

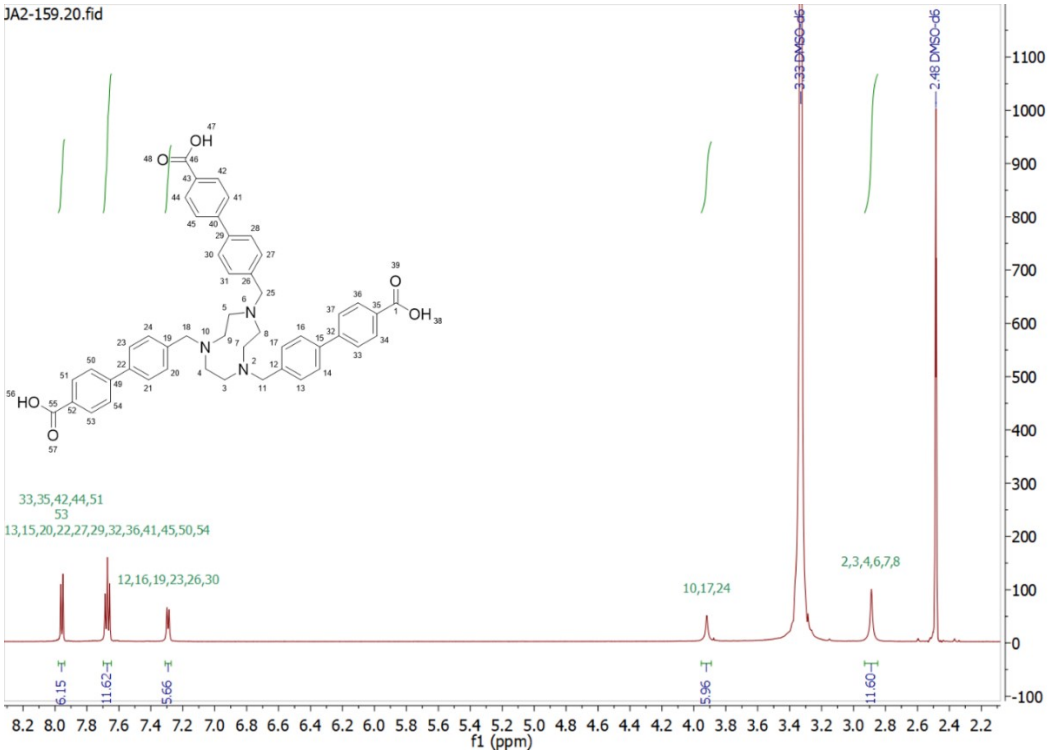

Figure S1. ^{1}H NMR spectra of $H_3$2·3HCl·2H_2O.

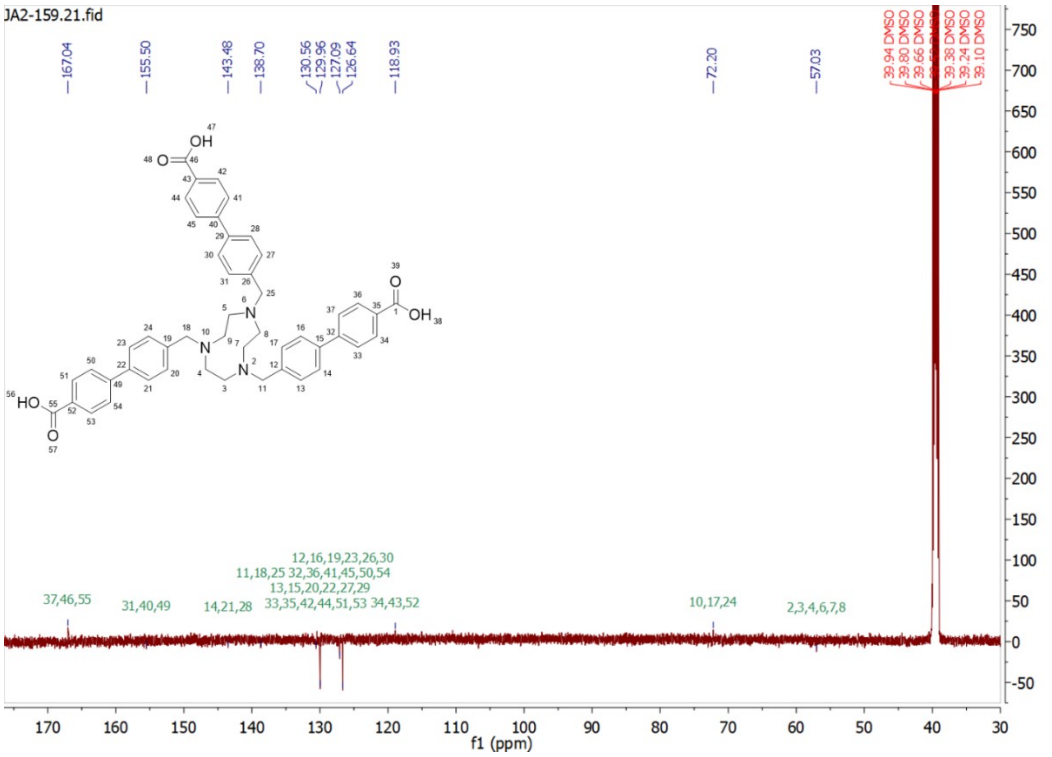

Figure S2. ^{13}C NMR spectra of $H_3$2·3HCl·2H_2O.

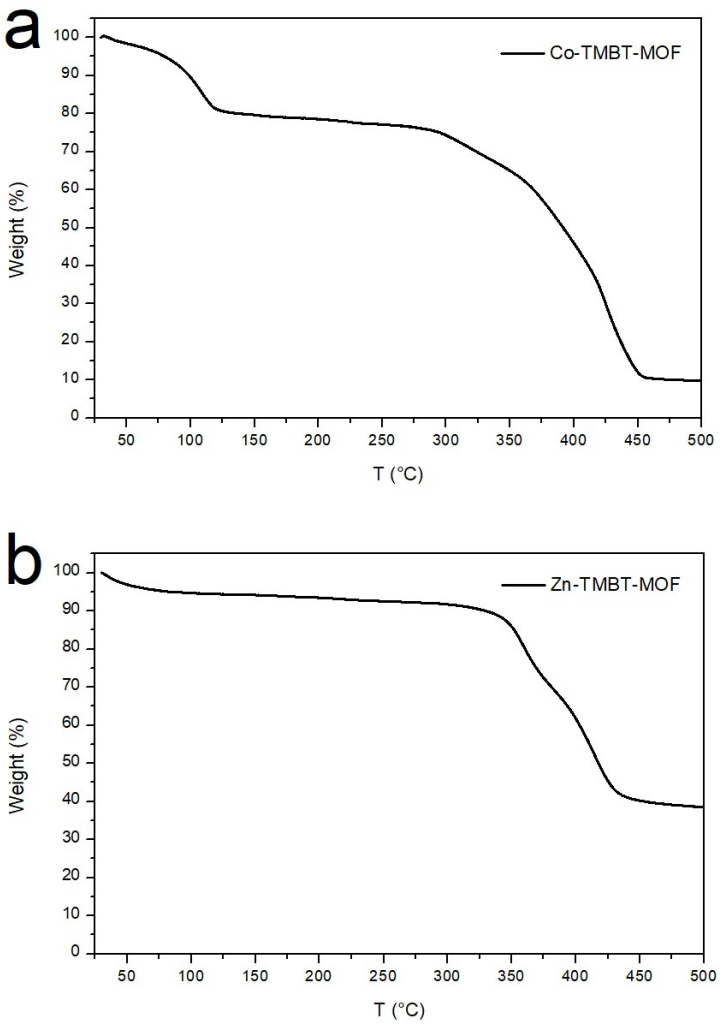

Figure S3. Thermogravimetric analysis of as-synthesized a) **Co-TMBT-MOF** and b) **Zn-TMBT-MOF**.

2. Crystallographic Details

Identification code	**Co-TMBT-MOF**	**Zn-TMBT-MOF**
Empirical formula	$C_{51}H_{54}CoN_4O_9$	$C_{55.5}H_{74.5}ClN_{5.5}O_{16}Zn_2$
Formula weight	1053.05	1240.89
Temperature/K	123.00(10)	100(2)
Crystal system	monoclinic	trigonal
Space group	$P2_1/n$	$R\text{-}3c$
a/Å	11.16580(10)	30.933(4)
b/Å	31.0750(3)	30.933(4)
c/Å	15.70250(10)	74.300(15)
α/°	90	90
β/°	95.0970(10)	90
γ/°	90	120
Volume/Å^3	5426.87(8)	61568(21)
Z	4	36
ρ_{calc}/g cm^{-3}	1.130	1.205
μ/mm^{-1}	2.907	0.802
F(000)	2228	23436
Crystal size/mm^3	0.2 × 0.15 × 0.1	0.1 × 0.08 × 0.05
Radiation	Cu Kα (λ = 1.54184)	Synchrotron (λ = 0.7108)
2Θ range for data collection/°	8.02 to 155.116	1.874 to 50
Index ranges	-14 ≤ h ≤ 12, -34 ≤ k ≤ 39, -19 ≤ l ≤ 19	-36 ≤ h ≤ 36, -35 ≤ k ≤ 35, -88 ≤ l ≤ 88
Reflections collected	110024	233727
Independent reflections	11436 [R_{int} = 0.0949, R_{sigma} = 0.0391]	12064 [R_{int} = 0.0809, R_{sigma} = 0.0257]
Data/restraints/parameters	11436/0/593	12064/0/480
Goodness-of-fit on F^2	1.044	1.203
Final R indexes [I≥2σ(I)]	R_1 = 0.0833, wR_2 = 0.2331	R_1 = 0.1022, wR_2 = 0.3061
Final R indexes [all data]	R_1 = 0.0944, wR_2 = 0.2447	R_1 = 0.1246, wR_2 = 0.3322
Largest diff. peak/hole / e Å^{-3}	0.83/-0.60	1.18/-0.44
CCDC	2220214	2220213

Co-TMBT-MOF: No restraints were applied to the structural model. The Solvent Mask routine in Olex2 was used to account for electron density that could not be modelled, calculating 72 e$^-$ in 331 Å^3 per asymmetric unit (equivalent to per formula unit). This is assigned as 1 x DMF and 3 x H_2O (calculated 70 e$^-$), in reasonable agreement with TGA and elemental analysis.

Zn-MOF: The aromatics rings were refined using the SHELX AFIX 66/65 commands. It is clear that there is some rotational disorder, although this could not be modelled and the anisotropic atomic models accurately describe the system. Zn2A/B was modelled as disordered using a freely refining variable (22:78 occupancy). The Solvent Mask routine in Olex2 was used to account for electron density that could not be modelled, calculating 180 e$^-$ in 869 Å^3 per asymmetric unit (equivalent to per formula unit). This is assigned as 1 x Cl^-, 2.5 x DMF and 6.5 x H_2O (calculated 182 e$^-$), in reasonable agreement with TGA and elemental analysis.

3. Characterisation Data

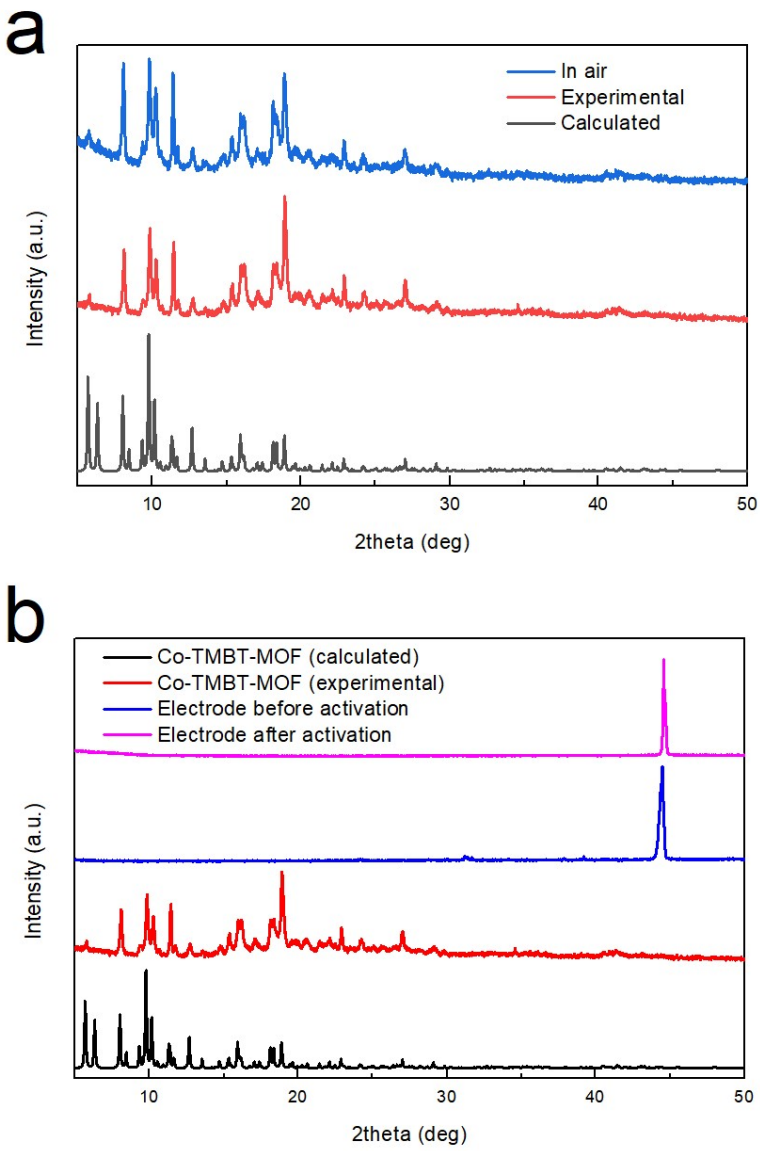

Figure S4. PXRD characterisation of **Co-TMBT-MOF**: (a) calculated data (*black*), experimental data obtained as synthesized (*red*) and after leaving exposed to air for 24 h (*blue*), (b) diffractograms recorded for the **Co-TMBT-MOF**/NF electrode before (*blue*) and after (*magenta*) 20 h OER test at 20 mA cm^{-2} in 1 M KOH at 23 ± 2 °C.

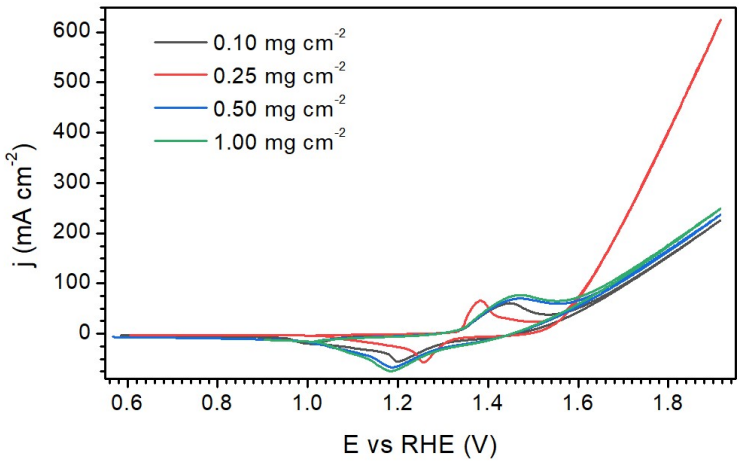

Figure S5. Electrocatalytic OER performance of Ni foam electrodes modified with **Co-TMBT-MOF** with loading levels varied from 0.10 to 1.00 mg cm^{-2} in 1 M KOH at 23 ± 2 °C in quasi-stabilised cyclic voltammetry measurements (scan rate 0.005 V s^{-1}; 10^{th} scans),

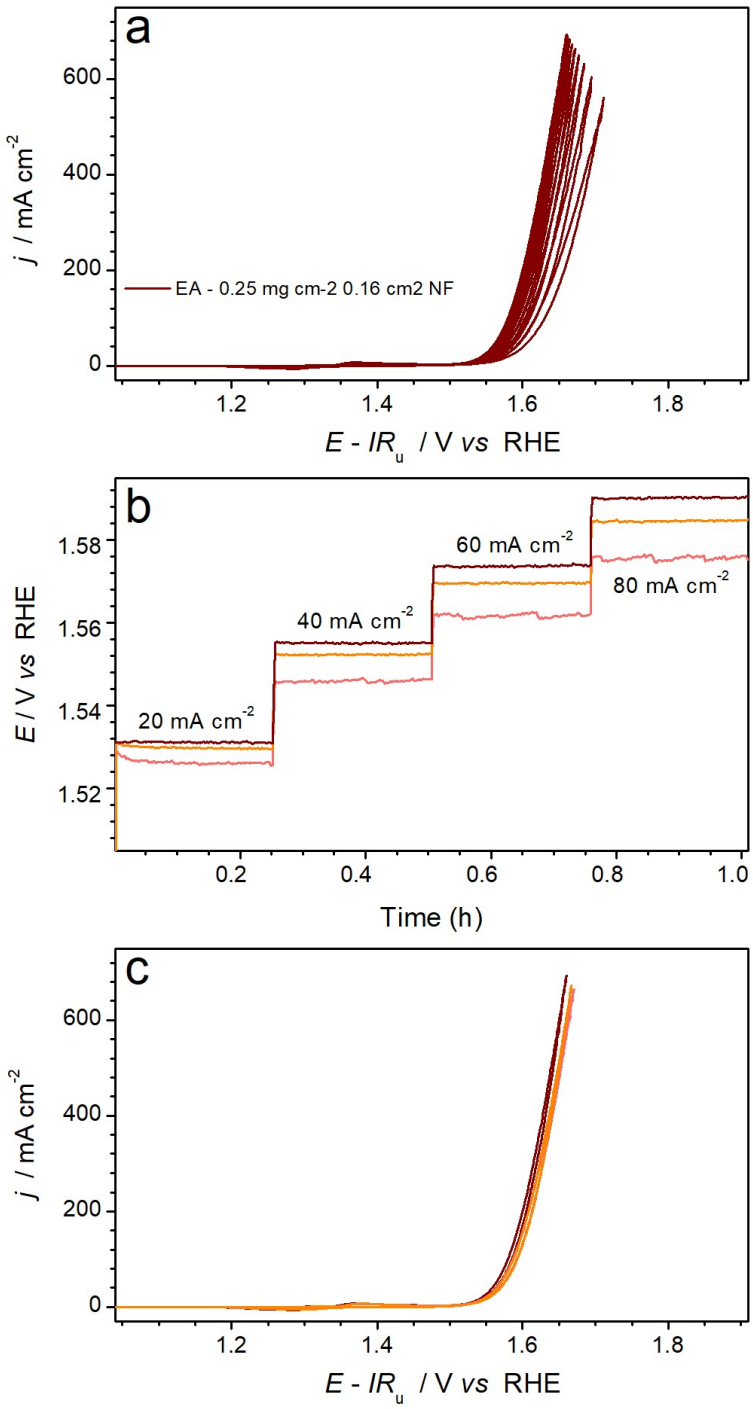

Figure S6. Electrocatalytic OER performance of Ni foam electrodes modified with **Co-TMBT-MOF** (0.25 mg cm^{-2}) in 1 M KOH at 23 ± 2 °C: (a) quasi-stabilised cyclic voltammetry measurements (scan rate 0.005 V s^{-1}; 10 scans), (b) multicurrent chronopotentiometric plot at increments of 20 mA cm^{-2} per 15 min for tests of three independent samples, and (c) cyclic voltammograms (scan rate 0.005 V s^{-1}; 10th stabilised scans) of three independent samples.

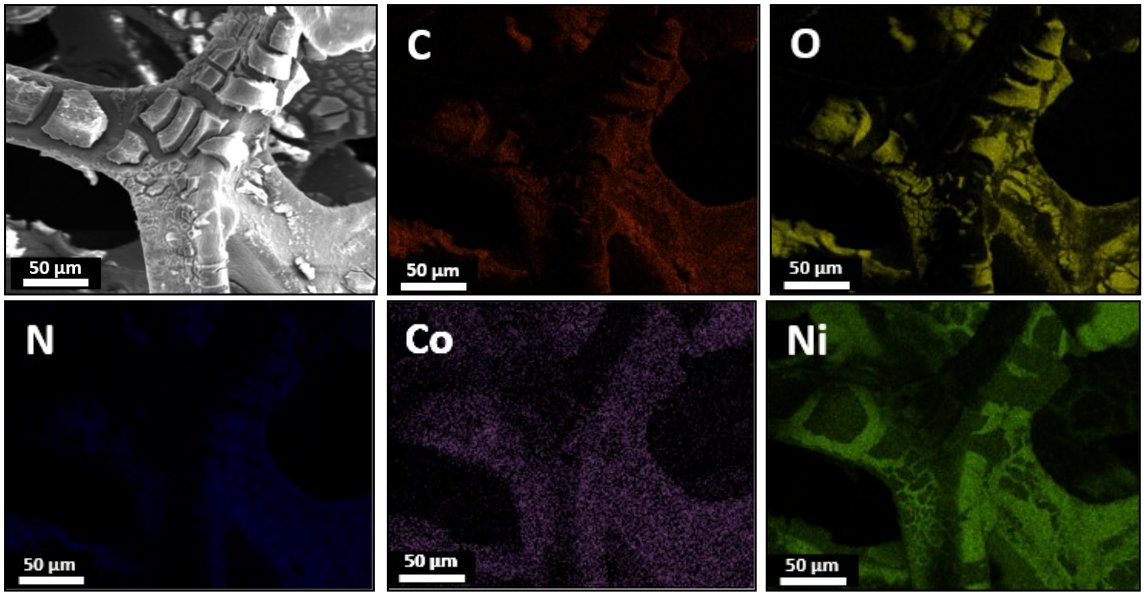

Figure S7. SEM/EDS elemental mapping of **Co-TMBT-MOF**/NF after 20 h OER test at 20 mA cm^{-2} in 1 M KOH at 23 ± 2 °C.

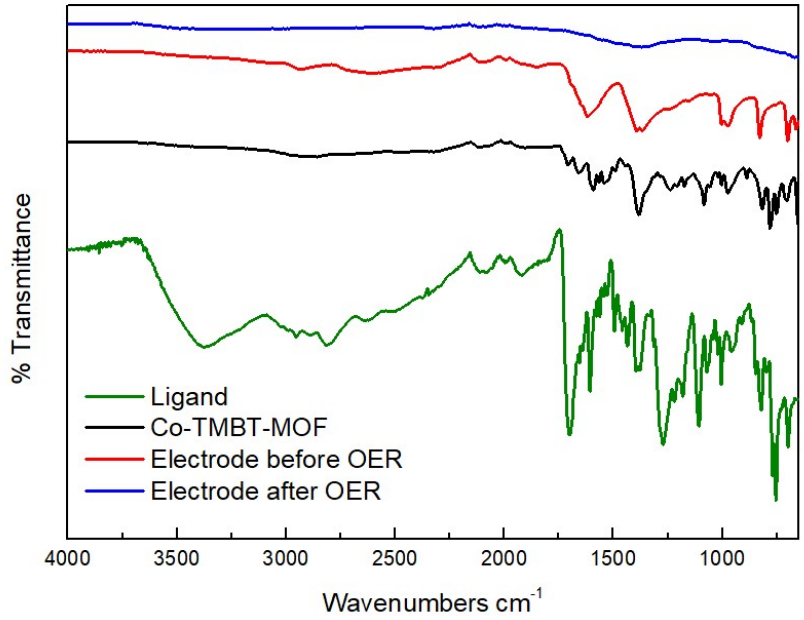

Figure S8. FTIR spectra of **$H_3$2·3HCl·2H_2O** (*green*), **Co-TMBT-MOF** (*black*), and **Co-TMBT-MOF**/NF electrode before (*red*) and after (*blue*) 20 h OER test at 20 mA cm^{-2} in 1 M KOH at 23 ± 2 °C.

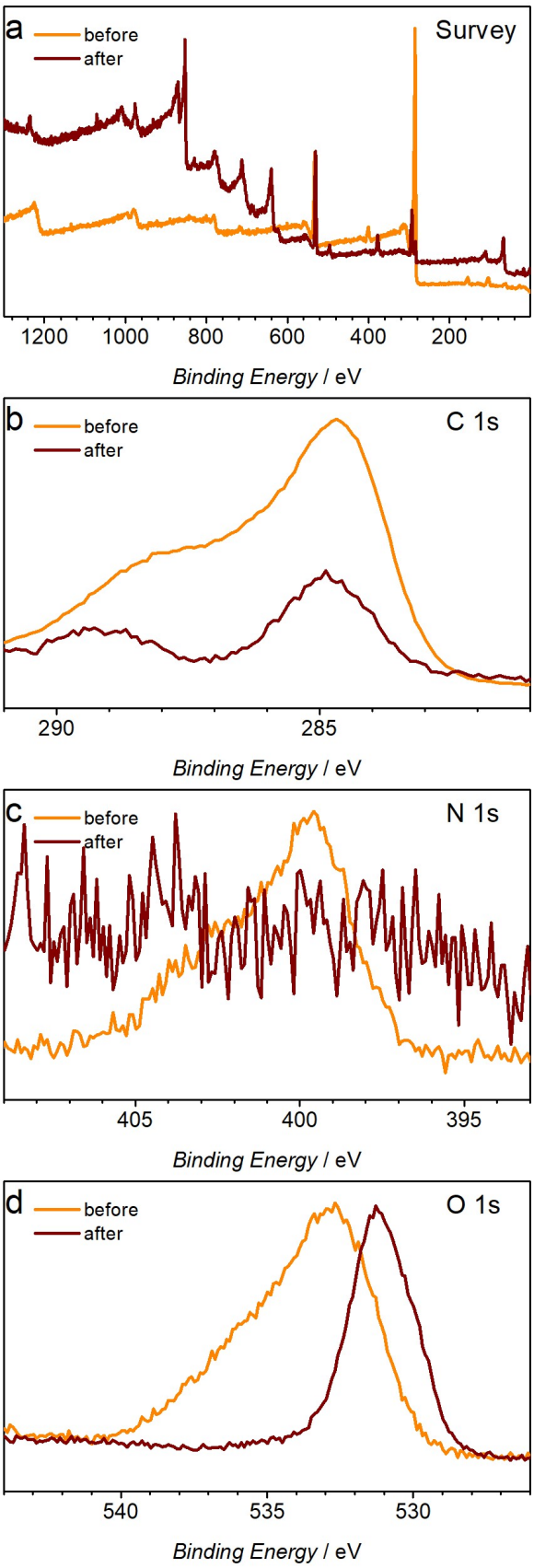

Figure S9. XPS characterisation of **Co-TMBT-MOF**/NF electrodes before (*orange*) and after (*brown*) 20 h OER test at 20 mA cm^{-2} in 1 M KOH at 23 ± 2 °C: (a) survey, (b) C 1s, (c) O 1s, and (d) N 1s spectra.

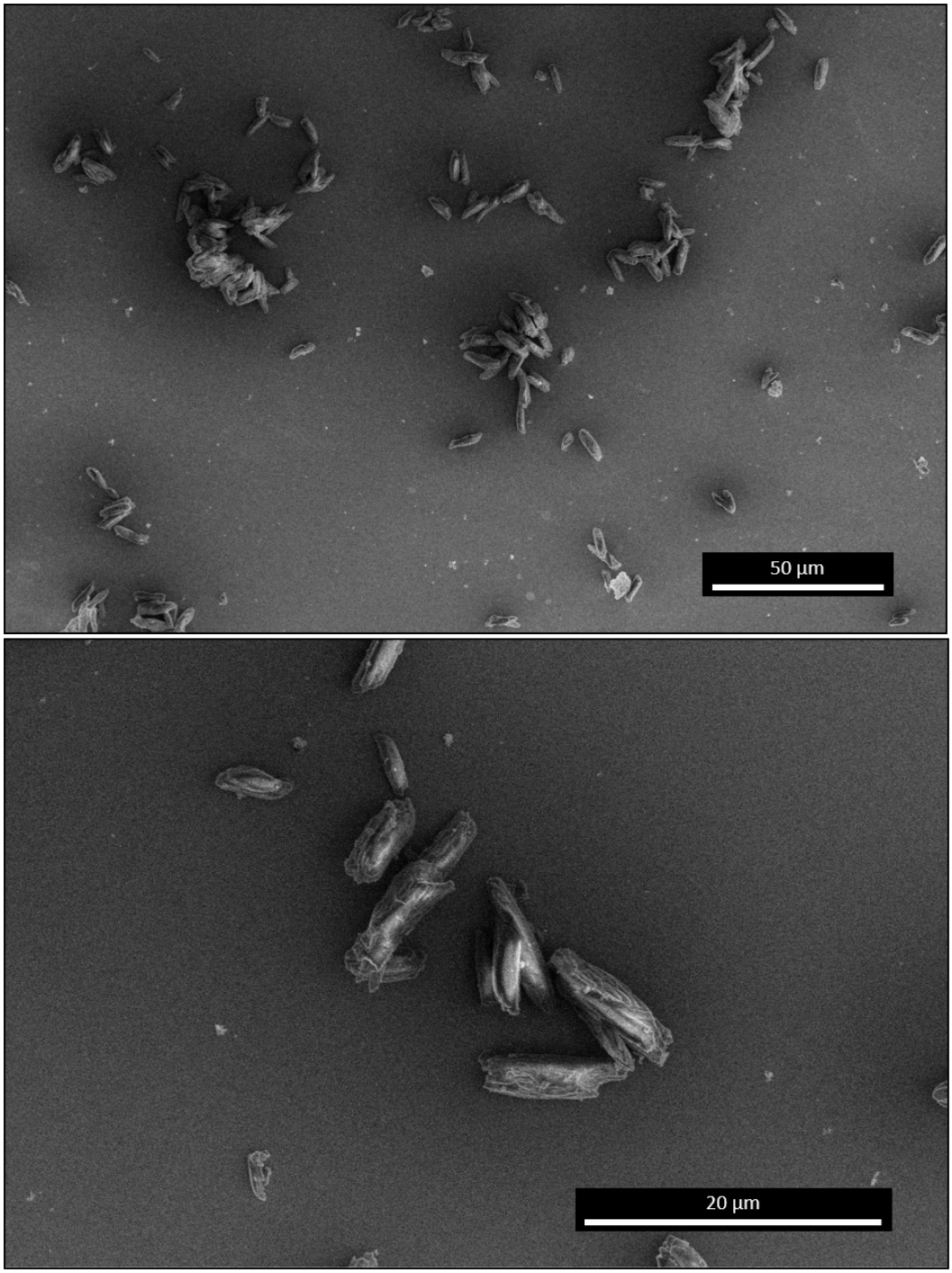

Figure S10. SEM images of the as-synthesised Co-TMBT-MOF on a Si wafer at different magnifications.

4. Comparison of Co-MOF-Derived Electrocatalysts

Table S1. Electrocatalytic performance of different materials derived from Co-MOFs for the OER in 1 M KOH at ambient temperature.

MOF	Ligand	Substrate[a]	MOF loading / mg cm^{-2}	OER current density / mA cm^{-2} at a specified OER overpotential / V	Tafel slope / V dec^{-1}	Ref
Co-TMBT-MOF	1,4,7-Tris(4'-methylbiphenyl-4-carboxylic)-1,4,7-TACN	NF	0.25	20 at 0.29 ± 0.01	53	Present study
Co-BPDC-MOF (*in-situ*)	Biphenyl-4,4'-dicarboxylic acid	NF	4.33	20 at *ca* 0.29	74 [b]	[1]
Co-BPDC-MOF (powder)	Biphenyl-4,4'-dicarboxylic acid	NF	Not reported	20 at *ca* 0.40	109 [b]	[1]
Fe-BTTA-MOF	2,5-bis(1H-1,2,4-triazol-1-yl) terephthalic acid	CFP	0.50	10 at *ca* 0.38	Not reported	[2]
FeCo-BTTA-MOF	2,5-bis(1H-1,2,4-triazol-1-yl) terephthalic acid	CFP	0.50	10 at *ca* 0.30	42 [b]	[2]
FeCo-BTTA-MOF	2,5-bis(1H-1,2,4-triazol-1-yl) terephthalic acid	NF	0.50	10 at *ca* 0.23	42 [b]	[2]
Fe/Co(1:2)-BDC-MOF	1,4-benzenedicarboxylic acid	GC	Not reported	10 at *ca* 0.31	Not reported	[3]
Co-BTC-BIm-MOF	benzene tricarboxylic acid, benzimidazole	GC	0.25	10 at *ca* 0.28	Not reported	[4]
$(Ni_2Co_1)_{0.925}$-$Fe_{0.075}$-MOF	1,4-benzenedicarboxylic acid	NF	0.54	10 at *ca* 0.26	Not reported	[5]

[a] NF, nickel foam; CFP, carbon fiber paper; GC, glassy carbon. [b] Derived from non-steady-state voltammetric data.

References

1. J. Yu, Y. Cao, Q. Liu, Y. Luo, Y. Liu, X. Shi, A. M. Asiri, T. Li and X. Sun, *ChemNanoMat*, 2021, **7**, 906-909.
2. J. Tian, F. Jiang, D. Yuan, L. Zhang, Q. Chen and M. Hong, *Angew. Chem. Int. Ed.*, 2020, **59**, 13101-13108.
3. K. Ge, S. Sun, Y. Zhao, K. Yang, S. Wang, Z. Zhang, J. Cao, Y. Yang, Y. Zhang, M. Pan and L. Zhu, *Angew. Chem. Int. Ed.*, 2021, **60**, 12097-12102.
4. R. K. Tripathy, A. K. Samantara and J. N. Behera, *Dalton Trans.*, 2019, **48**, 10557-10564.
5. Q. Qian, Y. Li, Y. Liu, L. Yu and G. Zhang, *Adv. Mater.*, 2019, **31**, 1901139.